

# New photon-counting detectors for single-molecule fluorescence spectroscopy and imaging

X. Michalet<sup>a\*</sup>, R. A. Colyer<sup>a</sup>, G. Scalia<sup>a</sup>, S. Weiss<sup>a</sup>  
 Oswald H. W. Siegmund<sup>b</sup>, Anton S. Tremsin<sup>b</sup>, John V. Vallerga<sup>b</sup>  
 F. Villa<sup>c</sup>, F. Guerrieri<sup>c</sup>, I. Rech<sup>c</sup>, A. Gulinatti<sup>c</sup>, S. Tisa<sup>d</sup>, F. Zappa<sup>c</sup>, M. Ghioni<sup>c</sup>, S. Cova<sup>c</sup>  
<sup>a</sup> Department of Chemistry & Biochemistry, UCLA, Los Angeles, CA  
<sup>b</sup> Space Sciences Laboratory, UCB, Berkeley, CA  
<sup>c</sup> Dipartimento di Elettronica de Informazione, Politecnico di Milano, Milano, Italy  
<sup>d</sup> Micro Photon Devices, Bolzano, Italy

## ABSTRACT

Solution-based single-molecule fluorescence spectroscopy is a powerful new experimental approach with applications in all fields of natural sciences. Two typical geometries can be used for these experiments: point-like and widefield excitation and detection. In point-like geometries, the basic concept is to excite and collect light from a very small volume (typically femtoliter) and work in a concentration regime resulting in rare burst-like events corresponding to the transit of a single-molecule. Those events are accumulated over time to achieve proper statistical accuracy. Therefore the advantage of extreme sensitivity is somewhat counterbalanced by a very long acquisition time. One way to speed up data acquisition is parallelization. Here we will discuss a general approach to address this issue, using a multispot excitation and detection geometry that can accommodate different types of novel highly-parallel detector arrays. We will illustrate the potential of this approach with fluorescence correlation spectroscopy (FCS) and single-molecule fluorescence measurements. In widefield geometries, the same issues of background reduction and single-molecule concentration apply, but the duration of the experiment is fixed by the time scale of the process studied and the survival time of the fluorescent probe. Temporal resolution on the other hand, is limited by signal-to-noise and/or detector resolution, which calls for new detector concepts. We will briefly present our recent results in this domain.

**Keywords:** photon-counting, detector, single-molecule, fluorescence, spectroscopy, imaging

## 1. INTRODUCTION

The need to detect single-molecules arises in multiple fields[1-3]. In basic science, elucidating the steady-state characteristics of heterogeneous mixtures or studying intrinsically stochastic molecular mechanisms requires observing one molecule at a time and reproducing this observation with a statistically significant number of different molecules to sample a large parameter space. In biomedical diagnosis or drug screening, the ability to rapidly test for the presence of a chemical agent or reaction using minute amount of materials is of paramount medical but also economical importance. Single-molecule detection is also the only way to detect rare events or rare molecular conformations. This capability is of direct relevance to the field of ultrasensitive detection of pathogens or chemicals, due to its ultimate sensitivity.

Single-molecule detection can be achieved using different physical effects, but optical means in particular have the advantage of allowing non-destructive detection and being usable with different sample states (gaseous, liquid, solid) and experimental arrangements (flow, diffusion, surface). Several types of spectroscopic signatures can be used to distinguish different molecular species and most can be used at the single-molecule level: fluorescence emission spectrum, polarization or polarization anisotropy, lifetime, Raman spectrum, etc.

Single-molecule detection by optical means requires two different conditions to be fulfilled:

- (i) The signal (photons) from a single molecule needs to large enough be detectable by the photon sensor;
- (ii) Signals from different molecules need to be distinguishable.

The first criterion (*detectability*) has two facets, due to the fact that one has to deal with very weak signals (either a small number of photons or a very small relative change of total number of photons). From a detector point of view, it

---

\* michalet@chem.ucla.edu

means that sensitivity needs to be maximized and readout noise minimized. From a sample point of view, it means that the quantum yield of the optical process to be detected needs to be maximized. It also requires the ability to separate signal from background (and if this is not feasible, background needs to be minimized).

The second criterion (*separability*) is a bit more general and complex to discuss exhaustively within the scope of this article. In essence, molecules can be distinguished only if they have different optical signatures and/or they are sufficiently separated spatially and/or temporally[4].

Before discussing detector requirements, it is worthwhile briefly examining typical geometries that can be encountered in single-molecule fluorescence detection, which we will do in the next two sections. Section 2 will discuss solution-based point-like geometries, while Section 3 will be devoted to widefield detection geometries and their applications. Section 4 will present recent developments in multipixel detectors enabling high-throughput single-molecule measurements. Section 5 will describe recent advances in widefield photon-counting detectors towards better performance single-molecule imaging and spectroscopy. We conclude this article with a brief overview of future prospects for the field.

## 2. SINGLE-MOLECULE DETECTION AND SPECTROSCOPY IN POINT-LIKE GEOMETRIES

### 2.1. Single-molecule burst detection

A simple way to fulfill the separability criterion in fluorescence spectroscopy is by ensuring that the region in which molecules are excited is small enough and the concentration of molecules low enough such that there is at most one molecule in it at any given time (Fig. 1A). In other words, if the minimum achievable excitation volume is  $V_x$ , the molar concentration  $C$  needs to be such that  $C \ll (N_A V_x)^{-1}$  .where  $N_A$  is Avogadro's number.

A standard approach to achieve point-like excitation is by tightly focusing collimated laser light in the sample. The achievable diffraction-limited volume (defined using the full-width at half-maximum (FWHM) of the point-spread function (PSF) of the instrument) is then of the order of[5]:

$$V_x \sim \lambda^3 NA^4, \quad (1)$$

where  $\lambda$  is the excitation wavelength and  $NA$  is the numerical aperture of the lens. Using standard values for these parameters ( $\lambda = 532$  nm,  $NA = 1.2$ ), one obtains a typical diffraction-limited excitation volume of a fraction of a femtoliter ( $1 \text{ fl} = 10^{-15}$  liter =  $1 \mu\text{m}^3$ ) and the requirement that the concentration be significantly smaller than a few nanomolar (nM). This concentration requirement is not always easy to achieve or even desirable, for instance when the sample cannot be diluted (e.g. when making observations inside a live cell), or because low concentration would reduce the rate of occurrence of the process to be detected (large dissociation constants).

Different techniques have been developed to further reduce excitation volumes and thus increase the range of accessible concentrations to larger values (e.g. near-field excitation[6], stimulated emission depletion[7], zero-mode

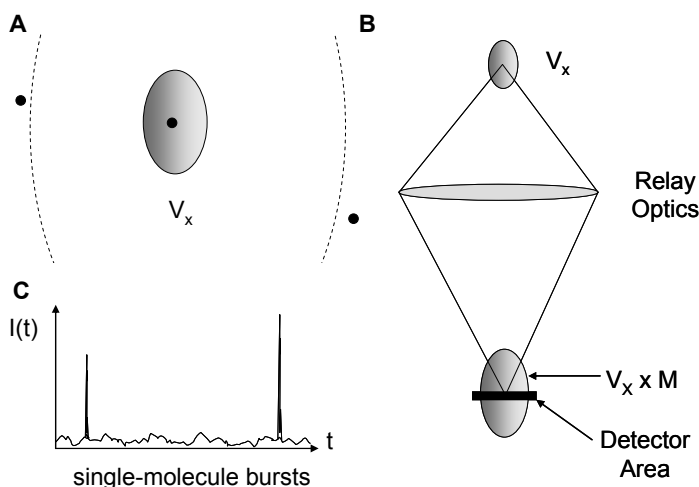


Fig. 1. A: Single-molecule burst detection requires at most one molecule at any given time in the excitation volume  $V_x$ . B: For optimal single-molecule signal-to-background ratio, the detector sensitive area needs to be of the order of the size of the PSF image. C: The resulting signal consists of brief bursts corresponding to the transit of a single-molecule through the excitation volume.

wave guides[8], etc) but in general they add complexity to the experiment. We will limit ourselves in this section and Section 4 to confocal microscopy, which uses a laser light source and a high numerical aperture objective lens to focus excitation light and collect emitted fluorescence[5]. Its advantage is its simplicity and its ability to detect signals relatively deep into a liquid sample ( $\sim 100\ \mu\text{m}$ ) through a standard thickness glass coverslip ( $\sim 150\ \mu\text{m}$ )[9].

Creating a small excitation volume is only the first step in single-molecule experiments. Efficient collection of the weak light emitted by individual molecules is also experimentally challenging. Due to the limited numerical aperture of conventional lenses (which translates in an opening angle  $< 180^\circ$ ) and losses in the additional relay optics and filters, collection efficiency is usually a few percent of the total emitted signal at best. It is thus critical to match the size of the image of the emission volume to that of the detector: too small a detector (or equivalently too large a magnification) will clip the image and result in loss of precious photons (Fig. 1B). On the other hand, the detector size cannot be increased arbitrarily, as otherwise background signal from outside the region of interest will be picked up (and additionally, detector dark noise will usually increase with detector area), decreasing the signal-to-background ratio (SBR). We will come back to this issue of detector versus PSF size when discussing high-throughput single-molecule applications.

When an adequate trade-off between these parameters is achieved, distinct photon bursts can be detected as signature of the brief transit of individual molecules across the excitation/detection volume (Fig. 1C). For diffusing molecules, burst duration depends on the molecule size, the solvent viscosity and the excitation volume. Typical values range from a few  $10\ \mu\text{s}$  to a few ms. Immobile molecules can be detected for longer periods of time using this geometry, but are usually observed using a widefield geometry as discussed in the next section.

Burst intensity depends on excitation power, fluorescence quantum yield of the molecule and detection efficiency and can reach a few hundreds photons. Due to emission saturation and photobleaching, increasing the excitation power is beneficial only up to a certain point, after which background increases faster than signal reducing the SBR. Additionally, since these are very weak signals, shot noise is a significant issue.

Obviously, the detector temporal resolution needs to be shorter than the burst duration (a few  $\mu\text{s}$  are usually sufficient for most experiments). Typical detectors used in these experiments are single-photon avalanche photodiodes (SPADs), photomultiplier tubes (PMTs) or hybrid photodetectors (HPDs). Photon-counting detectors are in fact almost indispensable due the very low signal which requires negligible readout noise (the readout noise of a photon-counting detector being zero). Better temporal resolution than that called for by the burst durations may be needed for time-correlated measurements, in which each photon is timed with respect to a reference signal (typically the exciting laser pulse) or other detected photons[10]. In this case, the temporal resolution needed depends on the typical time scale to be studied and may reach a few  $10^3$ 's of ps. We will not discuss this type of measurements in this section but will address it in section 5.

## 2.2. Single-molecule burst analysis

Detecting and characterizing bursts (by arrival time, duration and intensity) is only a preliminary step, which could be, in principle, considered part of the data acquisition process. It is rarely sufficient by itself, even for counting molecules, as artifacts and experimental sources of variability makes the relationship between number of counted bursts and actual number of molecules (or concentration) relatively uncertain. A built-in control or calibration is needed and is best provided by a two-channel measurement in which the number of events of interest detected is compared to that of a known control observed simultaneously in the same conditions. In more sophisticated schemes, each burst is comprised of two types of information, for instance two color intensities, and coincident detection is required to validate a count[11-12].

However, single-molecule burst detection can be used to perform more interesting measurements than mere counting when combined with various spectroscopic techniques. For instance, the conformation of a molecule (protein, nucleic acid, etc) or respective location of two interacting molecules can be studied by monitoring the distance between two dyes attached to specific sites of the molecule(s) using fluorescence resonant energy transfer (FRET). When the two dyes have overlapping absorption and emission spectra and are in close proximity, intermolecular non-radiative (resonant) energy transfer can occur by dipole-dipole interaction, with an efficiency varying with the 6<sup>th</sup> power of the distance between the two dyes[13]. This phenomenon has been extensively used in bulk, but its use at the single-molecule level (smFRET) has exploded since its first demonstration in 1996[14]. In smFRET experiments, doubly labeled molecules or molecular complex are excited by a single laser exciting the donor dye. The fluorescence signals from the donor and acceptor dyes are collected simultaneously in their respective emission band by two separate detectors (Fig. 2A). After identification of individual bursts, the donor and acceptor signals ( $I_D$  and  $I_A$ , Fig. 2B) are used to compute the FRET efficiency  $E \sim I_A/(I_D + I_A)$  which reports on the distance between donor and acceptor dyes via the Förster equation:

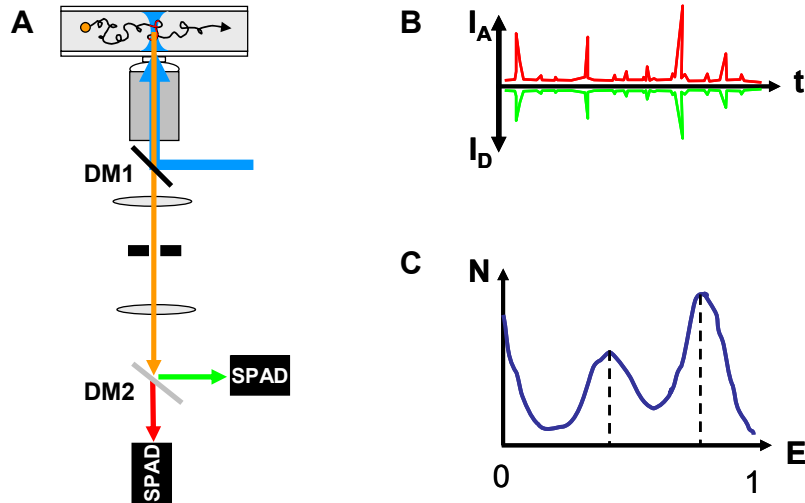


Fig. 2. A: Principle of confocal smFRET experiment showing a laser source (blue) focused into the sample by an objective lens, which also collects the emitted light (orange) separated from the excitation light by a dichroic mirror (DM1). Another dichroic mirror (DM2) separates the donor emission (green) from the acceptor emission (red), which are sent to two different detectors (SPAD). B: Each single-molecule burst is comprised of a donor component (green) and an acceptor component (red). C: The FRET efficiencies  $E$  of all bursts are histogrammed to uncover the different species (e.g. conformations) in equilibrium.

$$E = \left( 1 + \left( \frac{R}{R_0} \right)^6 \right)^{-1} \quad (2)$$

where  $R_0$  is a distance of the order of a few nanometers characterizing the donor/acceptor dye pair and its environment. The FRET efficiencies measured from multiple single-molecule bursts are then histogrammed (Fig. 2C) to identify populations of molecules characterized by particular  $E$  values, as well as their respective fraction. Refinements of this general technique have been developed to carefully analyze the contribution of shot noise to these distributions, or help identify molecules labeled with a donor only or acceptor only dye, using alternating laser excitations (ALEX)[12]. Their discussion is however beyond the scope of this article.

As mentioned previously, other types of spectroscopic signatures can be studied as well (polarization, lifetime) using variants of this setup. In particular, 3- or more color smFRET/ALEX measurements allow studying complex biochemical molecular assemblies, conformations and interactions[15].

This general experimental scheme is very sensitive but requires each burst to be separable from the next. Moreover, due to the random nature of diffusion, burst intensities are distributed quasi-exponentially, with very small intensity bursts representing the majority. Therefore, long acquisition times are required to obtain a sufficient number of large enough bursts to conduct precise quantitative measurements. This has two detrimental consequences:

- Long acquisitions (minutes to hours);
- It is limited to equilibrium measurements.

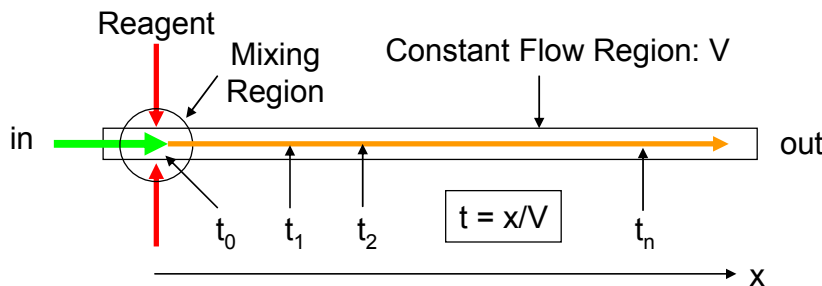


Fig. 3: Microfluidic arrangement for single-molecule stopped flow studies. Sample and reagents are rapidly mixed on one side of the device and flowed at a constant velocity toward the other end. Single-molecule measurements are performed at different locations along the channel, corresponding to different time points  $t_i$  in the reaction.

This last point means that fast irreversible reactions cannot be studied by this approach, as they are over before enough single-molecule measurements have been performed. In other words, only reactions whose typical time scale is longer than the minimum duration of a measurement (a few minutes or more) can be studied in this geometry.

Microfluidics offers a possible solution to this problem when the reaction to be studied can be synchronized by rapid mixing of reagents, such as when studying protein folding dynamics (Fig. 3) [16]. In this “continuous flow” mixer geometry, reagents and single-molecules are mixed *rapidly* in a small region and flowed downstream at a constant flow velocity  $V$ , establishing a steady-state situation: the reaction is effectively restarted at the same location each time a new molecule enters it. The mixing region corresponds to time  $t_0 \sim 0$  of the reaction, while any downstream point at a distance  $x$  from this region corresponds to time  $t = x/V$ . Studying the reaction dynamics therefore consists in sampling the steady-state conformations at different location  $x_i$  (i.e. time  $t_i$ ) as was described in Fig. 2. Once sufficient single-molecule burst statistics has been accumulated at a given time point, the measurement can be repeated for the next time point. Of course, due to the stochastic nature of biochemical reactions, molecules will be progressively desynchronized as one moves away from the mixing region, raising a number of interesting interpretation issues which go beyond the scope of this brief review. For the same reason as before, these measurements can be quite lengthy, calling for increased throughput approaches.

### 2.3. Fluorescence Correlation Spectroscopy (FCS)

A related but distinct experimental regime, illustrated in Fig. 4A, is encountered when the point-like excitation volume contains one or a few molecules *on average* at any time. In a confocal microscope, this situation corresponds to sample concentration of a few nM. In this regime, individual molecule bursts cannot be distinguished anymore and are replaced by a highly fluctuating signal centered on an average value (Fig. 4B).

Analysis of the autocorrelation function (ACF) of these fluctuations (hence the name fluorescence correlation spectroscopy or FCS given to this technique[17]) can yield physical as well as photochemical information (molecule size and concentration, blinking or binding/unbinding rates) about the diffusing molecules (Fig. 4C). This technique only gives exploitable information at very low concentration, the relative amplitude of the ACF being inversely proportional to the average number of molecules in the excitation volume  $V_x$ . On the other hand, too low a concentration (that is in practice, single-molecule concentration) results in most of the signal coming from uncorrelated inter-bursts signal, resulting in very noisy ACFs.

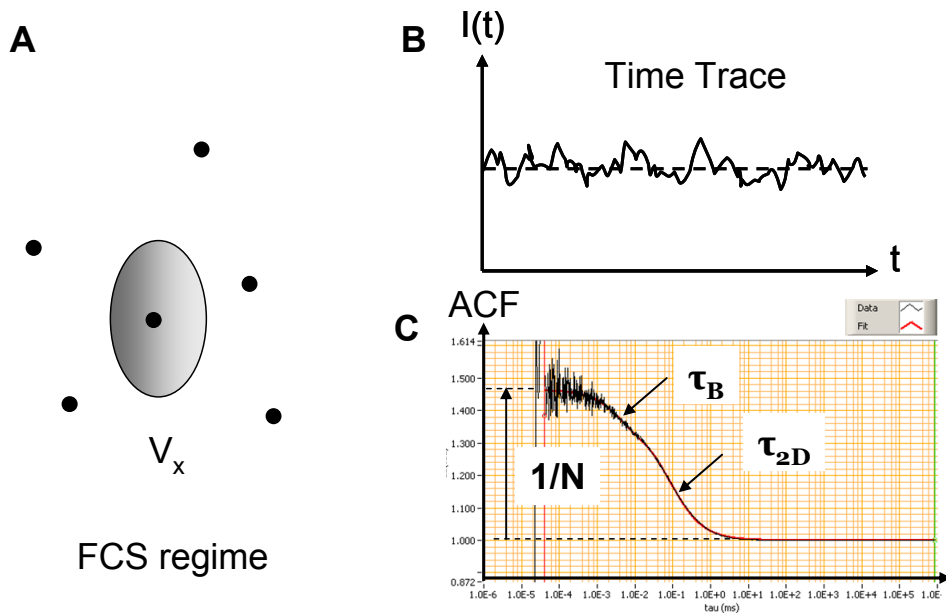


Fig. 4. A: FCS regime is characterized by a larger concentration of  $\sim 1$  or more molecules in the excitation volume  $V_x$  at any time. B: This larger concentration prevents from identifying single-molecule bursts in the signal time trace, which looks like a noisy, fluctuating signal (plain curve) around an average value (dashed line). C: The proper way to analyze this signal is by computing its autocorrelation function (ACF). Here a diffusing fluorescent dye sample results in a characteristic ACF curve exhibiting two typical time scale: a diffusion time  $\tau_{2D}$  and a blinking time scale  $\tau_B$ . The amplitude of the ACF gives access to the concentration ( $1/N$ ) of the sample.

For sensitive detection application, FCS techniques have the advantage of simplicity due to the existence of plug-and-play hardware correlators and the existence of well established data analysis methods. They are also capable of detecting populations of molecules with sufficiently different sizes, the ACF of a mixture being a weighted sum of the ACFs of each population[17].

As for single-molecule methods, multiple spectroscopic channels can be cross-correlated, including donor and acceptor emission in the case of a FRET experiment. Many sophisticated analysis schemes going beyond mere auto- or cross-correlation analysis of the signal have been developed, making this technique a very versatile approach to study millisecond to microsecond timescale inter or intramolecular dynamics.

The similarity with single-molecule methods extends to issues of detector size versus excitation/detection volume matching, signal-to-background, signal-to-noise ratio (SNR) and temporal resolution. Both techniques require:

- A very good detector quantum efficiency;
- An adequate match between the detector size and the excitation/detection PSF image size;
- A very good temporal resolution.

### 3. SINGLE-MOLECULE IMAGING AND SPECTROSCOPY

There are many experimental situations where the kind of point detection methods described above becomes inefficient. In particular, samples in which molecules diffuse slowly (as encountered for instance in cell membranes) or are immobilized on a surface, are not easy to study using point-like excitation/detection geometries.

Slowly diffusing molecules can be detected with point-like geometries as described before. In fact, since they stay longer in the excitation volume than fast diffusing species, the collected signal can be larger and easier to detect. However, it also takes longer for a new molecule to reach the excitation volume; therefore accumulating a statistically significant number of measurements takes more time (the concentration still needs to be very low to avoid having several molecules within the excitation volume). Also, the probability that the molecule photobleaches during its transit through the excitation volume is increased, potentially reducing the measurement yield.

Immobile molecules need to be first imaged and located, and finally positioned one at a time in the excitation volume (or the excitation volume moved to each different location sequentially). This is clearly a very inefficient sequential approach, with the additional disadvantages that imaging before data acquisition may result in premature photobleaching of molecules, and sample or setup drift may prevent from reliably analyzing more than a few molecules per image.

For those cases, an imaging approach using a widefield detector is more appropriate. In particular, since the observation time of each molecule can last as long as the molecule does not photobleaches, there is no need for a very high temporal resolution to simply detect the molecule, although it might be necessary to study fast dynamics.

Most widefield single-molecule experiments consist in taking movies of the sample, from which (multichannel) intensity time traces corresponding to individual molecules can be extracted (Fig. 5A). An imaging geometry has the advantage of allowing observing several molecules simultaneously, but also tracking them if they are mobile (Fig. 5B).

Similarly to point-like geometries but because of a different reason, there is a maximum concentration above which single-molecule analysis becomes impossible: it is attained when PSFs of nearby molecules overlap. For typical visible wavelength and numerical aperture, the corresponding density is of the order of 1 molecule per  $\mu\text{m}^2$  (or  $\mu\text{m}^3$  for 3D imaging). The total number of observable molecules is then set by the detector area, number of pixels and optics magnification.

Being able to simultaneously observe immobilized molecules for a long time simplifies the study of irreversible dynamics, since the number of independent measurements is equal to the number of molecules in the field of view. This geometry is also efficient to detect rare binding events, when one of the components can be surface immobilized.

Standard widefield detection uses cameras acquiring successive frames exposed for a finite period of time. Different sensor technologies and readout designs exist and are compatible with single-molecule detection, provided they meet a few performance requirements[18]:

- High sensitivity;
- Good temporal resolution;
- Low readout noise.

The first requirement is identical to that encountered in point detection. It is due to the unchanged fact that single-molecules emit very few photons and optics collection efficiency is usually limited to a few percents. CCDs, or to a lesser extent CMOS cameras, but also intensified cameras using different photocathode materials and amplification principles (e.g. image intensifiers based on phosphors or electron bombardment) are adequate for this task.

The second requirement is application-dependent (pure detection and/or counting, dynamic study) but more importantly, cannot be considered independently from the last one (readout noise). This is the main difference between

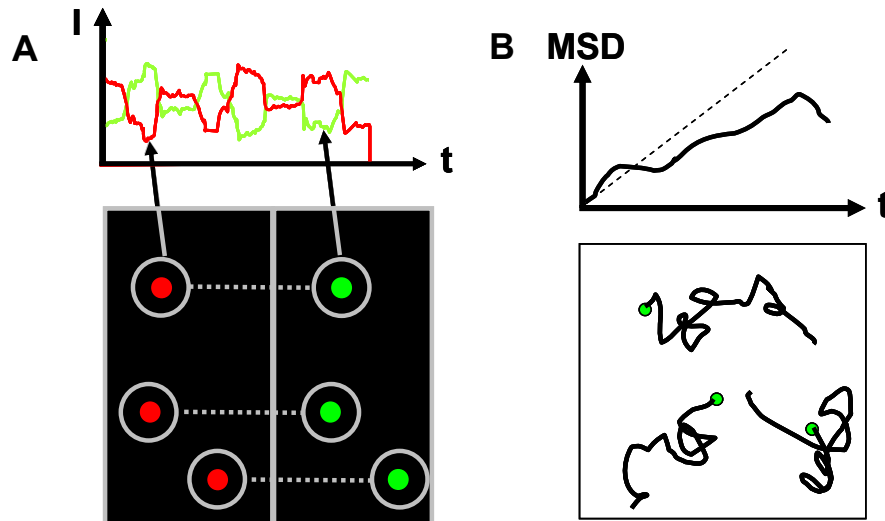


Fig. 5. A: Immobilized single-molecule FRET imaging. In this type of experiment, each donor/acceptor labeled molecule is immobilized on a glass surface and imaged in both donor and acceptor emission channels upon donor excitation. The corresponding intensities can be represented as single-molecule time traces (top), from which FRET efficiency dynamics can be studied. B: For mobile molecules, successive positions of each molecule can be determined with nm-resolution using single-particle tracking (SPT) algorithms. Analysis of the motion dynamics (e.g. using mean-square displacement –MSD analysis, top panel) allows determination of molecular parameters or information on their environment.

cameras and photon-counting devices used in point-like detection. Indeed, since single-molecule signals are very weak (not only in terms of the total number of photons, but also in terms of the achievable photon detection rate, typically lower than 100 kHz), it is mandatory to minimize the contribution of readout noise (expressed in  $e^-$  rms per pixel per frame) to preserve a sufficient SNR for the total signal per molecule *per frame*. In particular, due to the existence of readout noise, it is important to very carefully consider on how many pixels a single-molecule's PSF is imaged (large magnification or small pixel helps oversampling the PSF, which is useful to some extent for high-resolution localization applications such as superresolution imaging, but is paid for by a smaller SNR). Cameras with very low readout noise at large frame rates (such as scientific CMOS) or with no effective readout noise (such as electron multiplying CCD) are clearly advantageous for these applications.

With cameras, the minimum temporal resolution increases with the total number of pixels due to the way pixel values are digitized and/or transferred to memory. The exact value depends on the technology (full frame, interline or frame transfer readout for CCD technology, serial – CCD, or parallel –CMOS digitization), but is for most devices still in the ms range and above. As a reminder, due to readout noise, very high theoretical frame rates are in practice useless for single-molecule detection due to their small emitted signal. Moreover, time-correlated measurements of the type briefly mentioned in Section 2.1 are clearly impossible with such devices.

Finally, it is worth considering a serious drawback of standard widefield detectors at high frame rates: since single-molecule imaging is *sparse* imaging (due to the requirement to be able to distinguish each individual PSF), most of the pixels contain information unrelated to any single molecule (and for the most part just readout noise) and is thus wasted bandwidth and disk space.

We will discuss a novel detector concept designed to address most of these issues in Section 5.

#### 4. NEW STRATEGIES FOR HIGH-THROUGHPUT SINGLE-MOLECULE SPECTROSCOPY

Parallelization is the simplest way to address the throughput limitations of point-like detection. This problem was in fact initially encountered in fast confocal imaging and has received a number of technical solutions in the past. Single-molecule detection brings some peculiarities that make some of these solutions inadequate. Parallelization is challenging because it needs to address four separate but inter-related issues:

- Sample excitation parallelization;
- Signal detection parallelization;
- Excitation and detection alignment;
- Data processing parallelization.

We will briefly discuss these points, before presenting some of the solutions we have explored.

#### 4.1. Sample excitation parallelization

Multispot excitation can be obtained using different approaches (cascaded beamsplitters, microlens arrays, diffractive optics element, spatial light modulators, etc). The practical requirements are that each spot needs to be sufficiently separated from its neighbors to avoid cross-talk (signal excited by one spot is detected by a neighboring detector). A simple rule of thumb is that the spot separation,  $l$ , needs to be at least a few times their diameter (Fig. 6)[19]. The spot size itself is defined based on the excitation PSF, which to first approximation can be modeled as a slightly elongated 3D Gaussian along the optical axis. Noting  $\sigma_{xy} \sim 0.21 \lambda/NA$  the PSF's standard deviation in the focal plane, the above criterion can be expressed as  $l > d \sim 6 \sigma_{xy}$ . In practice larger separation may be needed to account for high sample concentration or large detector area (see below).

#### 4.2. Signal detection parallelization

The detector pitch,  $L$ , divided by the optical magnification,  $M$ , needs to match the spot separation,  $l$ . Since the minimum spot size  $d$  is fixed by the focusing optics ( $NA$ ) and excitation/emission wavelength ( $\lambda$ ), this previous constraint also fixes the ratio  $\delta = D/Md$  (detector size in PSF unit or *reduced detector size*). As discussed in Section 2, this is an important parameter in both single-molecule burst detection and FCS applications, for which the optimal values are different, although of the order of one. In other words,  $d$  being fixed by the excitation optics and sample characteristics, choosing the spot separation fixes the pitch to size ratio (or *aspect ratio*,  $\alpha = L/D$ ) of the detector. The magnification  $M$  can then be adjusted to ensure that the optimal reduced detector size  $\delta$  is used.

It is noteworthy that the condition  $l > d$  results in  $L > D$ , which means that the *fill factor* of an ideal detector for single-molecule spectroscopy,  $\pi(D/L)^2 = \pi\alpha^{-2} < 1$ , a requirement that distinguishes these applications from traditional imaging applications, for which a fill factor as close to 1 as possible is generally sought for (and sometimes obtainable using an apposed lens array).

#### 4.3. Excitation and detection alignment

Determining the correct optical parameters for an optimal match between excitation and detection is only the

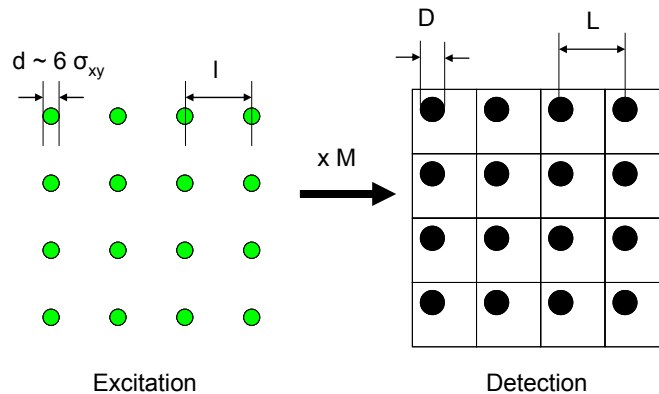


Fig. 6: Multispot excitation and detection geometry requirements. A: on the excitation side, spots need to be separated by at least the PSF dimension  $d$ . B: on the emission side, the detector pitch  $L$  needs to match that of the spot times the magnification,  $L = Ml$ , while the relation between detector and spot size depends on the specific application.

first step in actually ensuring that single-molecule signals will be efficiently collected. The next step consists in aligning the multiple excitation volumes with their respective detector pixels. Since detector pixel size is in the range of 10 to 100  $\mu\text{m}$ , a task that is relatively easy to accomplish *at the single pixel level* with standard micrometer-resolution translation stage is rendered challenging by the introduction of one or more additional degrees of freedom *for multipixel detectors*, corresponding to the different possible orientations of the detector. This additional alignment complexity can be easily solved using a programmable pattern generator allowing complete control on the position, scale and orientation of the excitation pattern. Using a direct space pattern generation approach (in contrast to holographic approaches) makes it

straightforward to either interactively or automatically orient and shift, as well as adjust the pitch of simple patterns, as we have recently demonstrated with 1D and 2D patterns using a *liquid crystal on silicon spatial light modulator* (LCOS SLM)[20]. Some challenges remain when trying to align *several* multipixel detectors to a common excitation pattern, as encountered in multicolor detection needed for smFRET experiments.

#### 4.4. Parallel data processing

The raw data from a single-photon detector consists of digital pulses that can be time-tagged, binned or counted, processed to detect bursts and extract different related quantities (e.g. FRET efficiency). In FCS, the intensity time trace is auto-correlated (or cross-correlated with other signals), while in time-correlated applications, precise timing information needs first to be extracted using time-to-digital converters (TDC) and then histogrammed and fitted to decay models. The computational cost of these tasks grows linearly with the number of pixels and can become rapidly taxing for a personal computer in terms of CPU, RAM and disk space. Efforts to offload some or all of these tasks to *digital signal processors* (DSP), *field programmable gate arrays* (FPGA) or *graphics processor units* (GPU) will be needed to allow real-time data analysis and representation for more than a few channels.

#### 4.5 Results

We have recently demonstrated single-molecule burst detection and FCS analysis with an 8-pixel linear custom-technology SPAD array (Fig. 7A-B)[20-21] and a 32×32 pixels CMOS SPAD array (1K SPADA, Fig. 7C)[22]. In these experiments, a 532 nm pulsed laser ( $P > 1$  W) and an LCOS SLM with relay optics were used to generate a linear or square array of diffraction-limited spots with software-adjustable pitch and orientation.

The custom-technology detector is comprised of eight  $d = 50$   $\mu\text{m}$  diameter SPADs arranged in a linear fashion (pitch  $l = 250$   $\mu\text{m}$ )[23]. Their quantum efficiency peaks at 550nm (50 %) and reaches 48 % at 580 nm, the emission peak of Rhodamine 6G (R6G) used in these experiments. The TTL signals generated by each SPAD upon photon detection were fed to a reconfigurable (FPGA) digital input board programmed to detect pulses and associate a time-tag to each of them (12.5 ns resolution). Data was transferred asynchronously to a computer, which saved it on disk and was used for data processing (time trace binning and ACF calculation). We successfully demonstrated parallel FCS measurements from quasi-diffraction-limited spots separated by 5  $\mu\text{m}$  in a 1 nM sample. Calibration using a sample with known diffusion coefficient and concentration as a reference allowed renormalization of the ACF curves, resulting in limited dispersion of the fitted parameters (Fig. 7A). The same geometry was used to study a much less concentrated sample of

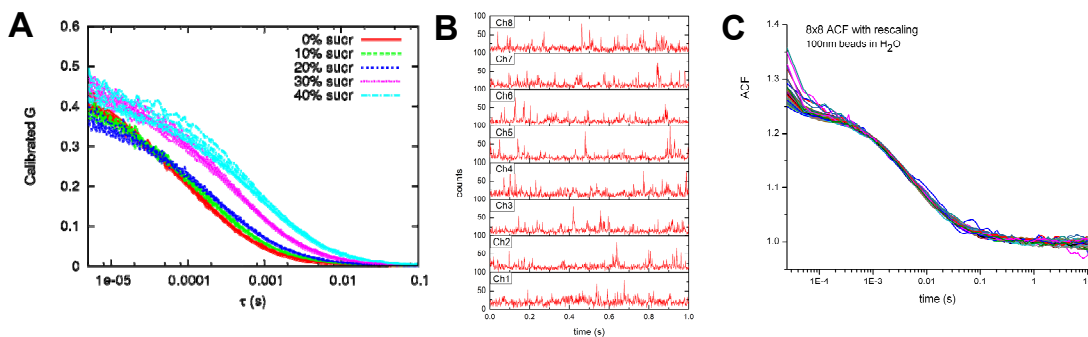


Fig. 7: High-throughput single-molecule spectroscopy and FCS. A: 8-channel FCS study of R6G in different concentrations of sucrose. After proper calibration, the data from different channel collapse on a common curve characteristic of the sucrose concentration. B: 8-channel, 1 ms binned time traces showing 50-100 kHz single R6G molecule bursts. C: 64-channel FCS study of 100 nm fluorescent beads. After calibration, all 64 curves collapse on the same characteristic function.

R6G (100 pM), for which clear single-molecule burst could be identified on each separate channel (Fig. 7B).

The CMOS SPAD array is comprised of 1024  $d = 20$   $\mu\text{m}$  diameter SPADs arranged in a square matrix (pitch  $l = 100$   $\mu\text{m}$ )[24]. Their quantum efficiency peaks at 460 nm (40 %) and reaches  $\sim 20$  % at 580 nm, the center of the band pass filter used in these experiments. Each pixel is equipped with its own quenching electronics, 8 bit counter and latch memory, allowing counting to proceed while the array is read out. The array function is controlled by an FPGA board containing 32 MB of memory and a USB communication module for data transfer to the host computer. The 8 KB content of the full array can be read in 10  $\mu\text{s}$  into onboard memory. Limiting the bit depth of each counter or the size of

the region of interest allows faster readout rates. An additional bandwidth limitation exists due to USB transfer, effectively limiting continuous acquisition of data with lossless transfer to the computer to  $\sim 20$  MB/s.

Due to the lower sensitivity and larger dark count rate of this detector, detection of single-molecule bursts turned out to be challenging. Moreover, although we could generate up to  $32 \times 32$  excitation spots in the sample using a 40X oil immersion objective lens ( $NA = 1.4$ ), the out-of-focus light generated by this large number of spots resulted in significant background signal in FCS measurement, leading to low amplitude ACF curves. We successfully demonstrated  $8 \times 8$  spots FCS analysis of bright 100 nm diameter fluorescent beads. After correction for channel differences, the 64 calibrated curves nicely collapse to a single master curve (Fig. 7C).

These experiments are as interesting for their positive as for their negative results. In particular, using a large number of spots seems to necessitate large spot separation to limit background signal due to out-of-focus excitation. This, of course, requires correspondingly large pixel separation for the detector (i.e. smaller fill factor). It is also worth noting that large spot numbers call for significant input laser power. For instance, a 1024 spot excitation pattern will typically require  $1024 \times 100 \mu\text{W} \sim 100$  mW at the sample level. In our LCOS SLM approach, which requires expanding the laser beam in order to uniformly cover the LCOS array, this necessitates significantly larger input power. Finally, time-tagging each detected photon results in transferring large amounts of data to the computer. For a typical sample with  $\sim 30$  kHz of average signal per spot, an (efficient) 32 bits encoding scheme per photon results in a  $\sim 1$  MB/s data rate for 8 channels. The data rate for binned data as provided by the 1K SPADA is even larger when used at full capacity.

## 5. NEW DETECTORS FOR SINGLE-MOLECULE IMAGING

To address the lack of temporal resolution and time-correlated measurement capabilities of standard cameras, we have begun the development of a series of advanced widefield photon-counting detectors[25-30]. Their design is based on a large area (18-25 mm diameter) microchannel plate photomultiplier (MCP-PMT) head followed by a position sensitive anode (PSA) providing  $\sim 50 \mu\text{m}$  spatial resolution. Like a PMT, its sensitivity is mainly limited by the photocathode QE. Our first generation prototype (H33D Gen I) used a multi-alkali photocathode with a maximum QE of 10 % at 400 nm, while our more recent SuperGen II photocathode device (H33D Gen II) achieves a QE  $\sim 15\%$  in the visible range. The detector is capable of better than 100 ps temporal resolution (depending on the readout design), a local count rate ranging from 10 kHz (Gen I) to 100 kHz (Gen II) and a global count rate ranging from 500 kHz (Gen I) to several MHz (Gen II).

Spatial and temporal information for each photon is processed and encoded by an FPGA board, which also ensures asynchronous data transfer to the host computer. Custom software saves, processes, displays and provides tools to analyze the data. For instance, single quantum dots (QD) can be imaged with adjustable temporal resolution (Fig. 8A), even with the relatively low sensitivity of the Gen I detector[29]. Using pulsed laser excitation, time-correlated single-photon counting (TCSPC) analysis can be performed, as demonstrated with a moving QD aggregate in Fig. 8B[29]. Finally, extending this type of analysis to the whole field of view, fluorescence lifetime imaging (FLIM) microscopy is possible, although the amount of information to process becomes prohibitive and is better handled using phasor analysis[26, 28].

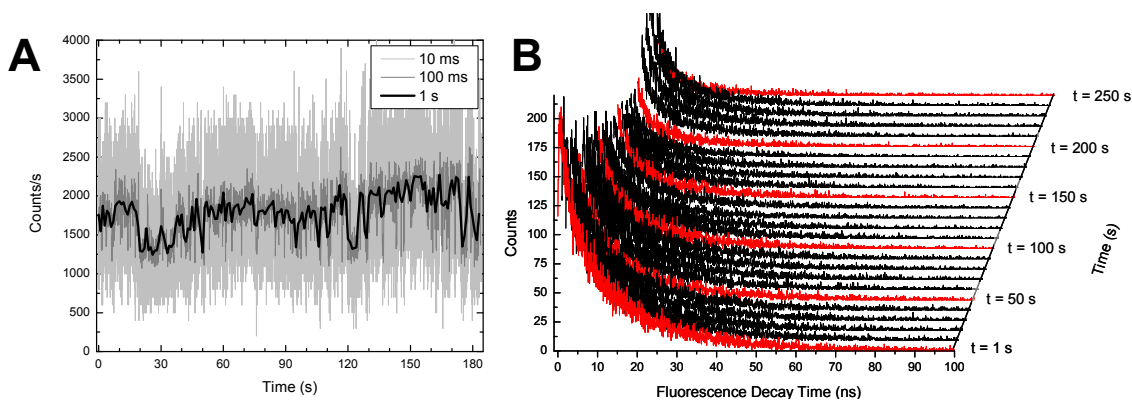


Fig. 8: H33D Gen I detector performance. A: Single QD time trace computed with different temporal resolution (1 s, 100 ms and 10 ms), showing the on/off blinking pattern characteristic of these quantum emitters. B: Fluorescence decay histograms obtained along the trajectory of a drifting QD aggregate. Each curve corresponds to 1 s of data sampled every 10 s along the trajectory (the raw data set contains a continuous recording of the trajectory).

## 6. CONCLUSION AND PERSPECTIVES

The preliminary results presented above are encouraging and suggest that significant throughput enhancement can and will be achieved in the near future. They also help better understand the essential requirements of single-molecule spectroscopy and imaging, which detectors need to achieve.

Detectors need to have the best possible quantum efficiency. For SPAD arrays, this calls in particular for enhanced sensitivity in the red part of the spectrum. Photocathode-based widefield detectors will benefit from using better sensitivity materials such as GaAs (visible and near infrared) or GaAsP (visible).

Photon-counting detectors do not have readout noise, but their dark count rate can be a problem for the low signal level characteristic of these applications. As a rule of thumb, for single-molecules emitting a detected count rate of 50 kHz, a maximum local dark count rate of a few kHz is tolerable (in fact, the sample *background* count rate is usually of this order of magnitude), although lower dark count rate is preferable. Since dark count rate scales with area, it is tempting to reduce it by decreasing the SPAD diameter, which has the added advantage of reducing cost. This is viable down to a certain point, as smaller SPADs require tighter focusing of the sample spot images and make alignment more challenging.

SPAD arrays current readout rate capabilities do not appear limiting for single-molecule spectroscopy, which rarely has to handle more than 100 kHz per spot. However, at large number of pixels, data throughput definitely appears as a possible issue due to the massive amount of data to save and process, even factoring in the decrease in total acquisition time allowed by parallelization. The most efficient strategy appears to perform most of the processing (burst detection and processing, ACF calculation, etc) before transfer to the computer. To be flexible, this kind of “intelligent sensors” will need to be easily reprogrammable by the user.

The widefield photon-counting detectors we are developing have some intrinsic limitations (maximum local count rate, maximum global count rate and simultaneous event handling capabilities) imposed by the laws of material physics and electronics design. New design principles will be required once the prototypes performance hit these hard limits. It is possible that large SPAD arrays coupled to microlens arrays to achieve fill factors close to 100% may be the best alternative solution.

Single-molecule imaging and spectroscopy raises a number of interesting challenges from a detector point of view, in both its point-like and widefield versions. We have presented our current efforts to take advantage of existing technologies to increase the throughput and information content achievable in these experiments. Clearly, a lot more needs to be done to reach optimal performance. What we have learned from our efforts is that a dialog between detector developers and single-molecule experimentalists is essential to optimize detector design and performance, and inversely, knowing the existing potential of detector technologies, suggests new types of more ambitious experiments. Some of the requirements of single-molecule imaging and spectroscopy overlap with a large number of other low-light level applications and therefore do not need a particular effort from the detector community to understand and address. Some however are rather specific and sometimes opposite to many standard applications (e.g. the low fill factor required for multispot single-molecule spectroscopy). However, the potential benefits of these technologies for biomedical, biopharmaceutical and biodetection applications in general will hopefully motivate more research and development of novel detectors, as well as funding for this type of activities.

## 7. ACKNOWLEDGMENTS

This work was supported by NIH Grant R01-EB006353 & R01-GM084327 and NSF Grant DBI-0552099 to UCLA & UCB and EC agreement 232359 (PARAFUO) FP7-SME-2008-1 to Politecnico di Milano.

## REFERENCES

1. Xie, X.S. and J.K. Trautman, *Optical Studies of Single Molecules at Room Temperature*. Annual Reviews of Physical Chemistry, 1998. **49**: p. 441-480.
2. Moerner, W.E. and M. Orrit, *Illuminating single molecules in condensed matter*. Science, 1999. **283**(5408): p. 1670-1675.
3. Weiss, S., *Fluorescence spectroscopy of single biomolecules*. Science, 1999. **283**(5408): p. 1676-1683.
4. Betzig, E., *Proposed method for molecular optical imaging*. Optics Letters, 1995. **20**(3): p. 237-239.

5. Pawley, J.B., ed. *Handbook of Biological Confocal Microscopy*. 2 ed. 1995, Plenum Press: New York.
6. Betzig, E. and J.K. Trautman, *Near-Field Optics: Microscopy, Spectroscopy, and Surface Modification Beyond the Diffraction Limit*. Science, 1992. **257**: p. 189-195.
7. Kasper, R., et al., *Single-Molecule STED Microscopy with Photostable Organic Fluorophores*. Small, 2010. **6**(13): p. 1379-1384.
8. Levene, M.J., et al., *Zero-mode waveguides for single-molecule analysis at high concentrations*. Science, 2003. **299**(5607): p. 682-686.
9. Selvin, P.R. and T. Ha, eds. *Single-Molecule Techniques: A Laboratory Manual*. 1st ed. 2007, Cold Spring Harbor Laboratory Press.
10. Becker, W., *Advanced time-correlated single photon counting techniques*. Chemical Physics, ed. A.W.J. Castleman, J.P. Toennies, and W. Zinth. 2005, Berlin: Springer.
11. Li, H.T., et al., *Ultrasensitive coincidence fluorescence detection of single DNA molecules*. Analytical Chemistry, 2003. **75**(7): p. 1664-1670.
12. Kapanidis, A.N., et al., *Fluorescence-aided molecule sorting: Analysis of structure and interactions by alternating-laser excitation of single molecules*. Proceedings of the National Academy of Sciences of the United States of America, 2004. **101**(24): p. 8936-8941.
13. Lakowicz, J.R., *Principles of Fluorescence Spectroscopy*. 2 ed. 1999, New York: Plenum. 698.
14. Ha, T., et al., *Probing the interaction between two single molecules: fluorescence resonance energy transfer between a single donor and a single acceptor*. Proceedings of the National Academy of Sciences USA, 1996. **93**(13): p. 6264-6268.
15. Michalet, X., S. Weiss, and M. Jäger, *Single-molecule fluorescence studies of protein folding and conformational dynamics*. Chemical Reviews, 2006. **106**(5): p. 1785-1813.
16. Lipman, E.A., et al., *Single-Molecule Measurement of Protein Folding Kinetics*. Science, 2003. **301**(5637): p. 1233-1235.
17. Krichevsky, O. and G. Bonnet, *Fluorescence correlation spectroscopy: the technique and its applications*. Reports on Progress in Physics, 2002. **65**(2): p. 251-297.
18. Michalet, X., et al., *Detectors for single-molecule fluorescence imaging and spectroscopy*. Journal of Modern Optics, 2007. **54**: p. 239-282.
19. Michalet, X., et al., *High-throughput single-molecule fluorescence spectroscopy using parallel detection*. Proceedings of SPIE, 2010. **7608**: p. 76082D.
20. Colyer, R.A., et al., *High-throughput FCS using an LCOS spatial light modulator and an 8x1 SPAD array*. Biomedical Optics Express, 2010. **1**(5): p. 1408-1431.
21. Colyer, R.A., et al., *High-throughput multispot single-molecule spectroscopy*. Proceedings of SPIE, 2010. **7571**: p. 75710G.
22. Colyer, R.A., et al., *Ultra-high-throughput single-molecule spectroscopy with a 1024 SPAD*. Proceedings of SPIE, 2011. **7905**: p. 790503.
23. Rech, I., et al., *Multipixel single-photon avalanche diode array for parallel photon counting applications*. Journal of Modern Optics, 2009. **56**(2): p. 326 - 333.
24. Guerrieri, F., et al., *Two-Dimensional SPAD Imaging Camera for Photon Counting*. Ieee Photonics Journal, 2010. **2**(5): p. 759-774.
25. Michalet, X., et al., *Photon-Counting H33D Detector for Biological Fluorescence Imaging*. Nuclear Instruments & Methods in Physical Research A, 2006. **567**(1): p. 133-136.
26. Michalet, X., et al., *A space- and time-resolved single-photon counting detector for fluorescence microscopy and spectroscopy*. Proceedings of SPIE, 2006. **6092**: p. 60920M.
27. Michalet, X., et al., *Fluorescence lifetime microscopy with a time- and space-resolved single-photon counting detector*. Proceedings of SPIE, 2006. **6372**: p. 63720E.
28. Colyer, R., et al., *Phasor-based single-molecule fluorescence lifetime imaging using a widefield photon-counting detector*. Proceedings of SPIE, 2009. **7185**: p. 71850T.
29. Michalet, X., et al., *Single-quantum dot imaging with a photon counting camera*. Current Pharmaceutical Biotechnology, 2009. **10**: p. 543-557.
30. Tremsin, A.S., et al., *High Speed Multichannel Charge Sensitive Data Acquisition System With Self-Triggered Event Timing*. IEEE Transactions on Nuclear Science, 2009. **56**(3): p. 1148-1152.